# Correspondence

## Sub$\mu$m Registration of Fiducial Marks Using Machine Vision

M. Tichem and M. S. Cohen

*Abstract*— **Sub$\mu$m registration between circularly symmetric fiducial marks can be achieved simply by finding their centroids by fitting circles to distributed edge positions determined by the second-derivative zero-crossing method. However, because of diffraction fringes, substantial errors originating in the tilt of the microscope optical axis must be minimized.**

*Index Terms*— **Machine vision, sub$\mu$m registration, fiducial marks, microscopy, diffraction efforts**

### I. Introduction

The stringent demands on laser-fiber alignment tolerance ($\sim \pm 1\,\mu$m for single-mode fiber) cause substantial difficulty in the fabrication of the transmitter package of an optoelectronic subassembly. The usual approach to this problem involves activation of the laser, followed by movement of the fiber into a position yielding the peak accepted and transmitted optical power, with subsequent fixing of the fiber position [1]. Several authors have recently suggested that, particularly for simultaneous alignment of *arrays* of lasers and fibers, a preferred alignment procedure may involve an alternative *passive* method in which the laser is not activated; instead the alignment requirements are achieved with the aid of special registration features [2], [3].

A passive laser-fiber alignment procedure under study in this laboratory is based on the use of *fiducial marks,* which are incorporated into both the laser chip and a specially made fiber carrier during their fabrication [4], [5]. During this "index alignment" procedure, the laser chip and fiber carrier are moved so that the fiducial marks associated with them are registered with fiducial marks demarcated on the underside of a special glass *alignment plate;* the latter fiducial marks are appropriately positioned so that precise juxtaposition of the component- and alignment-plate fiducial marks leads to correct laser-fiber alignment. The registration process is carried out while viewing the fiducial marks through the alignment plate with a microscope. Fabrication of transmitter optical subassemblies based on these principles has been demonstrated [4], [5].

During the implementation of these procedures, an operator observed the fiducial marks with the aid of a microscope/video-camera system, and manually controlled the motorized stages that determined the relative positions of the laser chip and fiber carrier with respect to the alignment-plate fiducial marks. The desired juxtaposition of the appropriate fiducial marks could be easily carried out by this means, especially when computer control of the motorized stages was introduced [5]. However, it was recognized that if large-scale production were to be undertaken, it would be advantageous to employ machine-vision techniques to measure the misalignment of the fiducial marks in order to permit automation of the alignment procedure. For this reason, a study of the feasibility of the determination of the misalignment of fiducial marks to sub$\mu$m precision by machine-vision methods was initiated.

The results of this study are communicated in the present report. While there have been several previous publications describing measurements of image features to subpixel accuracy [6]–[8], to the authors' knowledge there have been no previous reports of machine-vision fiducial-mark registration measurements to sub$\mu$m precision.

### II. Experimental and Analytical Techniques

In the previous passive laser-fiber alignment studies [4], [5], cross-shaped fiducial marks were employed for ease of viewing by human operators. The laser chip or fiber carrier was translated until each member of a pair of solid crosses patterned on it was centered within a corresponding hollow cross on the alignment plate. However, for the machine-vision studies, circles rather than crosses were chosen because of their invariance under rotation; furthermore, it has been pointed out that circular fiducial marks are associated with relatively low digitization error in determination of the centroid position [9]. Using circular fiducial circles were centered within corresponding tori delineated on the alignment plate.

For the abstracted studies under discussion, test patterns comprising a solid circle and a torus were photolithographically defined on standard chromium photolithographic mask blanks. An offset between the centers of the two objects was deliberately included in some of these patterns. For the present experiments the circle was 300 $\mu$m in diameter, and the torus had an inner diameter of 600 $\mu$m with an outer diameter of 800 $\mu$m; three different patterns of this design were studied, having offset values of 0, 19.00 $\mu$m, and 43.1 $\mu$m (Fig. 1). The major object of the present study was the determination of the precision with which machine-vision techniques could be used to measure the known offsets of the test patterns.

The patterns were viewed with a microscope fitted with a high resolution (1320 pixel × 1055 pixel) CCD camera;[1] the particular magnification used in these experiments corresponded to 1 $\mu$m/pixel. The images from this camera were stored in a frame grabber, then uploaded to the mainframe computer, where image analysis was performed.[2]

Despite efforts made to provide uniform Köhler illumination and suppress back-reflections, nonuniformity in illumination across the field of view was observed, and was found to cause errors. For this reason, the first step taken in the image processing was a computational correction for illumination nonuniformity [10]. For this purpose a multiplicative correction factor was found by measurement of the grey values corresponding to a featureless, uniformly reflecting sample used as a standard; this correction factor was then applied to all test images.

A variety of methods for the determination of object and edge positions are discussed in the literature [6]–[8], [11]–[13]. For the

Manuscript received August 24, 1992; revised March 25, 1993. Recommended for acceptance by Associate Editor S. Peleg.

M. Tichem is with the Laboratory for Flexible Production Automation, Faculty of Mechanical Engineering and Marine Technology, Delft University of Technology, Delft, The Netherlands.

M. S. Cohen is with IBM, T. J. Watson Research Center, Yorktown Heights, NY 10598 USA.

IEEE Log Number 9401641.

[1] Megaplus camera, VIDEK, Canandaigua, NY.

[2] The IAX image-processing software package (IBM Corp., Bredford UK) was used, together with auxiliary programs written in REXX.

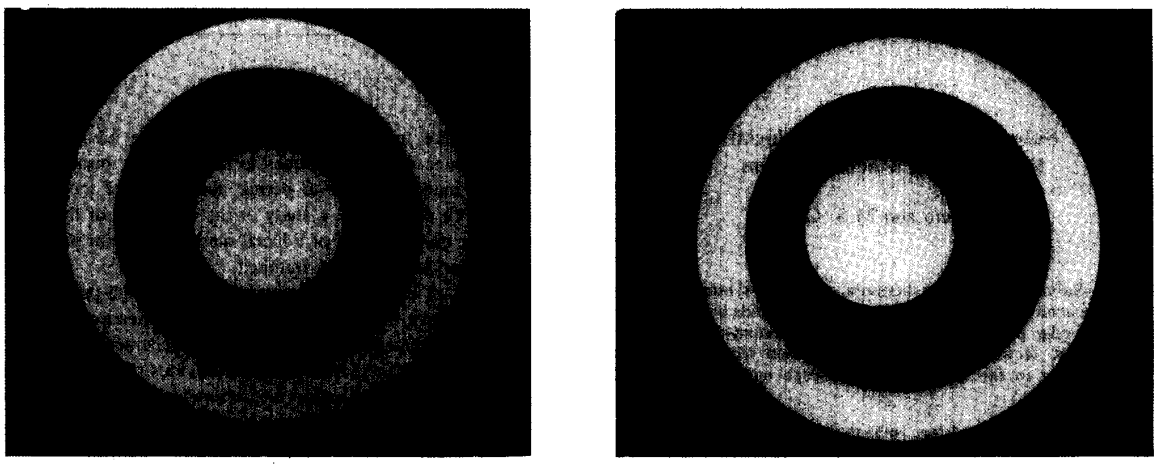

(a) (b)

Fig. 1. Test patterns with various values of offset between centroids of circle and torus. The patterns were delineated on standard chromium lithographic plates. Outer diameter of torus is $800\,\mu$m. (a) No offset. (b) $43.1\,\mu$m offset.

present application, the offset was computed from the corrected images by a simple three-step computation.

1) The two objects (circle and torus) were easily distinguished from the background by use of thresholding techniques, since the images were of high contrast. The position of the controids of the objects were then computed by calculating the first central moments (region analysis).[3] The resulting coordinates were considered first approximations, which were then used to obtain a second approximation of the object centroids.
2) Using the first-approximation centroids, radial intensity profiles were taken at 30 different azimuths, spaced at equal angular intervals around each object[4] (Fig. 2). The positions of edges of the object associated with the various azimuths were taken as the points where the second derivative of the grey value as a function of pixel position vanished.
3) The computed set of edge points was used to define a second approximation to the centroid coordinates. Several techniques were studied for this purpose. The preferred technique was based on the fact that the center of a circle is geometrically determined by three edgepoints; 10 sets of 3 points spaced 120° apart were used in these calculations, and the results averaged.[5]

[3]The area of each object was returned by the region-analysis program in units of pixel$^2$. The scale conversion factor ($\mu$m/pixel) was then calculated from this value and from the design value of the object diameter ($\mu$m).

[4]Operationally, the various intensity profiles were all obtained along the x axis by appropriately rotating the image, which, for the IAX software used, was possible only around a center specified by *integer* values of pixel coordinates. For this reason, in these calculations it was necessary to round off the centroid coordinates to integer values. Experiments showed that a choice of 30 such profiles was adequate; an increase in the number of profiles used did not lead to any appreciable increase in accuracy.

[5]Alternative techniques investigated were the following. 1) Simple averaging of the x, then the y coordinates of the edge points. 2) A four-point circle fit. 3) A least-square circle fit [14]. Technique 1 was comparatively inaccurate because of the angularly asymmetric distribution of edge points which originated in the fact that the chosen azimuths were based not on the true, but the first-approximation centroid. Techniques 2 and 3 gave good results, but the three-point circle fit technique was preferred because of its computational simplicity and low standard-deviation values.

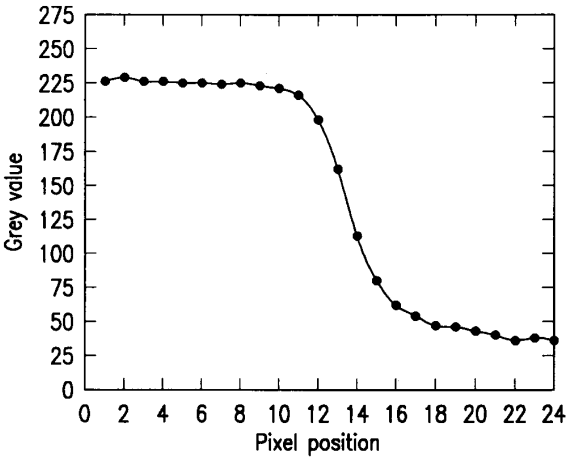


Fig. 2. Typical edge profile with large-aperture illumination.

## III. Experimental Results

In initial experiments on each of the three test patterns, several images associated with different positions and illumination conditions were analyzed by the methods described above. The resulting offset values exhibited large variations (standard deviation: $\sigma\sim$0.2-0.3 $\mu$m). Further investigation revealed the presence of diffraction fringes in the edge profiles (Fig. 3), particularly when a small aperture of illumination was used, i.e., under conditions of coherent illumination. It was found that a small tilt of the test-pattern normal with respect to the optical axis of the microscope caused an angular asymmetry in the position and intensity of the peaks of the diffraction fringes, which resulted in variations in the calculated edge positions. For this reason all subsequent experiments were conducted under large-aperture illumination conditions in order to suppress the illumination coherence; nevertheless, substantial diffraction-tilt effects still persisted.

It was therefore concluded that these effects could best be minimized by reducing the value of the tilt, i.e., by "leveling" the test pattern. An attempt was made to achieve adequate tilt suppression by reducing the illumination aperture in order to generate strong

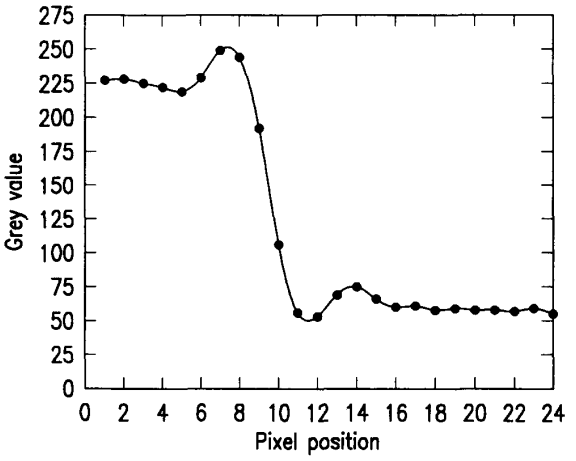


Fig. 3. Edge profile with highly coherent light (small illumination aperture) showing diffraction fringe.

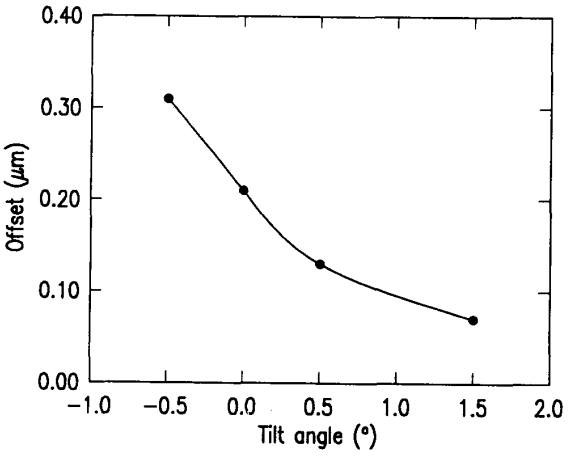


Fig. 4. Offset deviation vs. tilt angle for no-offset test pattern.

TABLE I
OFFSET DEVIATIONS FROM DESIGN VALUES

| Test Pattern | Design Value ($\mu$m) | Region Analysis 1st Approx ($\mu$m) | 3-Point Fit 2nd Approx ($\mu$m) |
|---|---|---|---|
| A | 0.0 | 0.52 | 0.21 |
| | | (0.038) | (0.040) |
| B | 19.0 | −0.37 | −0.14 |
| | | (0.034) | (0.39) |
| C | 43.1 | 0.63 | 0.39 |
| | | (0.021) | (0.000) |

diffraction fringes, then adjusting the levelling so that the fringes exhibited good angular symmetry; the illumination aperture was subsequently reopened before images were grabbed for analysis. Deviations of offset measurements from the design values are given in Table I for measurements on multiple images of each of the three test patterns; for each image the test pattern was repositioned and releveled. The standard deviation corresponding to each offset-deviation value is given in parentheses.

As anticipated, the 3-point circle-fit measurements (2nd approximation) yielded smaller deviation values than the region-analysis measurements. However, while all of the deviation values were sub$\mu$m, it was felt that an additional decrease in the deviation values and an additional reduction of the standard deviation would result from a further improvement in leveling.

For further study, the no-offset pattern was mounted on a special stage having orthogonal tilt axes in the horizontal plane, and the offset was measured at variaous tilt angles. It is seen (Fig. 4) that if the test pattern could be leveled to within $\pm 0.5°$, a mean value of offset $< 0.15\,\mu$m, with a corresponding $\sigma < 0.02$ $\mu$m would be expected. Since it is estimated that the positional error in fabrication of the test patterns was $\sim 0.1\,\mu$m, this result would be considered highly satisfactory.

Additional experiments with the no-offset pattern demonstrated that, starting from an arbitrary tilted condition, utilization of an iterative technique of offset measurement followed by releveling led to rapid convergence of the measured offset value to values $< 0.15\,\mu$m. This iterative technique could thus be used to eliminate tilt in the alignment plate of the passive laser-fiber alignment apparatus [4], [5], provided that a special concentric circle-torus pattern was delineated in the alignment plate; this tilt adjustment would be made only once, before machine-vision aided assembly operations began. Under these conditions, accurate machine-vision offset measurements unaffected by the tilt-diffraction phenomenon could subsequently be carried out during the assembly operations.

## IV. SUMMARY

The major obstacle to measurements of offsets to sub$\mu$m accuracy has been identified as diffraction effects compounded with object tilt with respect to the optical axis of the microscope. Provided that this tilt is first reduced to less than $\sim 0.5°$, e.g., by implementation of an iterative tilt-adjustment/offset-measurement technique, offset errors $< 0.15\,\mu$m with $\sigma < 0.02\,\mu$m may be anticipated with the use of circle-torus fiducial marks for a circle radius of $\sim 300\,\mu$m.

The image-analysis procedure found most effective for offset measurements includes: 1) Correction for illumination nonuniformity, 2) Finding the first approximation to the object centroids by region analysis, and 3) Finding the second approximation to the object centroids by identification of 30 distributed edgepoints using the second-derivative zero-crossing method, followed by 3-point fits to circles. These algorithms required long real-time intervals for the computer system that was used; a more practical implementation for a manufacturing application would be in hardware rather than software.

It may be noted that the offset-deviation values given above translate into about 0.15 pixel deviation with $\sigma$ of 0.02 pixel. These values may be compared with those obtained by Bose and Amir [9], who found that for a circular fiducial mark of 50 pixels diameter, the centroid could be determined to within a 0.1 pixel error with a $\sigma$ of 0.03 pixel. In the latter case large objects were studied under low magnification, so that diffraction-tilt effects were negligible.

## ACKNOWLEDGMENT

The authors thank R. S. Jaffe for guidance in developing the image-processing algorithms, F. W. Wu for providing the background-correction algorithm, D. S. Goodman for advice on optical problems, and R. Feigenblatt for assistance with video-camera problems.

## REFERENCES

[1] S. Enochs, "A packaging technique to achieve stable single-mode fiber to laser alignment," *Proc. SPIE*, vol. 703, pp. 42–47, 1986.

[2] C. A. Armiento *et al.*, "Passive coupling of InGaAsp/InP laser array and singlemode fibres using silicon waferboard," *Electron. Lett.*, vol. 27, pp. 1109–1110, 1991.

[3] K.P. Jackson *et al.*, "A compact multi-channel transceiver module using planar-processed optical waveguides and flip-chip optoelectronic components," in *Proc. 42nd ECTC*, 1992, pp. 93–97.
[4] M.S. Cohen *et al.*, "Packaging of laser-fiber arrays by index-alignment method," *IEEE Trans. Components, Hybrids, and Manufacturing Tech.*, vol. 15, Dec. 1992.
[5] ——, "Improvements in index alignment method for laser-fiber array packaging," *IEEE Trans. Comp., Hybrids Manuf. Technol. B*, to be published in vol. 17, Aug. 1994.
[6] C.A. Berenstein *et al.*, "A geometric approach to subpixel registration accuracy," *Comput. Vision, Graphics, and Image Processing*, vol. 40, pp. 334–360, 1987.
[7] Q. Tian and M.N. Huhns, "Algorithms for subpixel registration," *Comput. Vision, Graphics, and Image Processing*, vol. 35, pp. 220–233, 1986.
[8] S.S. Gleason *et al.*, "Subpixel measurement of image features based on paraboloid surface fit," *Proc. SPIE*, vol. 1386, pp. 135–144, 1991.
[9] C.B. Bose and I. Amir, "Design of fiducials for accurate registration using machine vision," *IEEE Trans. Pattern Anal. Machine Intell.*, vol. 12, pp. 1196–1200, 1990.
[10] F.W. Wu, private communication.
[11] P.D. Hyde and L.S. Davis, "Subpixel edge estimation," *Pattern Recognit.*, vol. 16, pp. 413–420, 1983.
[12] I. Overington and P. Greenway, "Practical first-difference edge detection with subpixel accuracy," *Image Vision Computing*, vol. 5, pp. 217–224, 1987.
[13] A.J. Tabatabai and O.R. Mitchell, "Edge location to subpixel values in digital imagery," *IEEE Trans. Pattern Anal. Machine Intell.*, vol. PAMI-4, pp. 188–201, 1984.
[14] S.M. Thomas and Y.T. Chan, "A simple approach for the estimation of circular arc center and its radius," *Comput. Vision*, vol. 45, pp. 362–370, 1989.

## Toward Object-Based Heuristics

Ari D. Gross

***Abstract*—Recovering the 3-D shape of an object from its 2-D image contour is an important problem in computer vision. In this correspondence, we motivate and develop two object-based heuristics. The structured nature of objects is the motivation for the nonaccidental alignment criterion: Parallel coordinate axes within the object's bounding contour correspond to object-centered coordinate axes. The regularity and symmetry inherent in many man-made objects is the motivation for the orthogonal basis constraint: An oblique set of coordinate axes in the image is presumed to be the projection of an orthogonal set of 3-D coordinate axes in the scene. These object-based heuristics are used to recover shape in both real and synthetic images.**

***Index Terms*—Shape from contour, object-based heuristics, nonparametric shape recovery, object recognition, perceptual organization.**

Manuscript received March 12, 1992; revised October 30, 1993. This work was supported by the National Science Foundation under Grant IRI-93-02041. Recommended for acceptance by R. Nevatia.

The author is with the Department of Computer Science, Queens College, City University of New York, Flushing, NY 11367–1597 USA, and the Center for Research in Intelligent Systems, Columbia University, New York, NY 10027 USA; e-mail: ari@vision.cs.qc.edu.

IEEE Log Number 9403159.

### I. Introduction

Shape from contour refers to methods in computer vision that use a single contour image to recover the shape of surfaces in the 3-D scene. This is an important problem in computer vision and one of the earliest considered by vision researchers. Although early work in the field focused on the rather restricted case of analyzing the line drawings of polyhedra, recent work has considered more general shape classes, such as right straight homogeneous generalized cylinders (SHGC's) [4], zero Gaussian curvature surfaces [12], and parametric shape models [8]. Despite recent progress in developing shape from contour methods for general shape classes, the current methods have their limitations. This correspondence motivates the need for *object-based heuristics* in general and then develops two specific object-based shape from contour methods.

In this correspondence, we are concerned only with image discontinuities resulting from the geometry of the viewed object. These geometry-related discontinuities are referred to as *contours*. Orthographic projection is assumed. Image contours correspond to a single object. Edge labeling, where required, is assumed to have been done *a priori*. Images are assumed to have been taken under *general viewpoint* conditions.

The term *object* in this correspondence refers to a collection of surfaces (one or more) that is naturally and efficiently described with respect to a global, orthogonal coordinate system. An example of an object is an ellipsoid, parameterized with respect to a set of three orthogonal coordinate axes determined by the intersection of its symmetry planes. Other examples of objects include SHGC's and Superquadrics, each of which is described with respect to an orthogonal, object-centered coordinate system. This definition for objects can include nonparametric shapes as well. A bilaterally symmetric planar object, for example, is naturally described with respect to the three axes determined by the intersection of the plane $P$ containing the surface, the symmetry plane $S$, and the transverse plane $T$ (perpendicular to both $P$ and $S$). One of the strong motivations, in fact, for using object-based heuristics is the ability to recover 3-D shape constraints from image contours without having a parametric model of the shape being recovered.

Previous work in the area of shape from contour is presented in Section II. In Section III, two object-based heuristics are developed. A nontrivial, real image example, using both heuristics, is presented in Section IV. Finally, conclusions and future work are discussed (Section V).

### II. Previous Work

We have divided previous shape from contour work into three categories: heuristics, parametric models, and perceptual organization methods. For reasons of conciseness, rather than critique specific heuristic methods as in [6], we present two problems with current heuristic techniques.

Consider the two vases shown in Fig. 1. The vase on the left is a regular circular vase, and the vase on the right is interpreted as an elliptical vase, i.e., a vase with an elliptical cross-section. The elliptical contour in Fig. 1(b) is not interpreted as the projection of a circle in $R^3$, because if the vase were a surface of revolution, the contour of the vase would have to be bilaterally symmetric, which it is not. Surfaces generally do not "stand alone"; i.e., an ellipse is not simply the projection of a circular planar figure floating in space, but rather, it is part of a larger object. Many surface-based heuristics,